

# Cationic Tris N-Heterocyclic Carbene Rhodium Carbonyl Complexes: Molecular Structures and Solution NMR Studies

Suzanne Burling,<sup>†</sup> Susie Douglas,<sup>†</sup> Mary F. Mahon,<sup>†</sup> Devendrababu Nama,<sup>‡</sup>  
Paul S. Pregosin,<sup>\*‡</sup> and Michael K. Whittlesey<sup>\*‡</sup>

Department of Chemistry, University of Bath, Claverton Down, Bath BA2 7AY, U.K., and  
Laboratory of Inorganic Chemistry, ETHZ, Hönggerberg, CH-8093 Zurich, Switzerland

Received March 2, 2006

The cationic N-heterocyclic carbene (NHC) rhodium complexes  $[\text{Rh}(\text{NHC})_3(\text{CO})]^+$  (NHC = ICy (**1**),  $\text{I}^i\text{Pr}_2\text{Me}_2$  (**2**)) have been isolated from the reactions of  $\text{RhH}(\text{PPh}_3)_3(\text{CO})$  with the free NHCs. The hexafluorophosphate salts of both compounds, **1** $[\text{PF}_6]$  and **2** $[\text{PF}_6]$ , have been characterized by X-ray diffraction. The observed temperature dependences of the  $^1\text{H}$  NMR spectra for **1** $[\text{PF}_6]$  and **2** $[\text{PF}_6]$  are a consequence of restricted rotation associated with the three  $\text{Rh}-\text{C}_{\text{NHC}}$  bonds. Line shape analyses from the NMR studies on **1** $[\text{PF}_6]$ , **1** $[\text{BAr}_4^{\text{F}}]$ , and **2** $[\text{PF}_6]$  ( $\text{BAr}_4^{\text{F}} = \text{B}(3,5-\text{C}_6\text{H}_3(\text{CF}_3)_2)_4$ ) afford activation barriers for the two trans-positioned  $\text{Rh}-\text{C}_{\text{NHC}}$  bonds of 35, 38, and 40  $\text{kJ mol}^{-1}$ , respectively. Pulsed-gradient spin-echo (PGSE) NMR measurements show that there is only a relatively small amount of ion pairing for these salts in dichloromethane solution.  $^1\text{H}-^{19}\text{F}$  HOESY data help to place the anions relative to the cations. Preliminary mechanistic studies on the formation of **1** and **2** suggest a role for neutral dinuclear precursors, as revealed by the reaction of  $(\text{PPh}_3)_2\text{Rh}(\mu\text{-CO})_2\text{Rh}(\text{I}^i\text{Pr}_2\text{Me}_2)_2$  with ICy, which affords the structurally characterized mixed NHC complex  $[\text{Rh}(\text{I}^i\text{Pr}_2\text{Me}_2)_2(\text{ICy})(\text{CO})][\text{PF}_6]$  (**3** $[\text{PF}_6]$ ).

## Introduction

Rhodium N-heterocyclic carbene (NHC) complexes have received considerable attention, principally due to the many important organic transformations that such species readily catalyze.<sup>1</sup> One of the advantages offered by NHCs compared to phosphines is that more subtle changes of stability and reactivity can be brought about through small variations of stereoelectronic effects. This has recently manifested itself in observations on stoichiometric processes of direct relevance to catalysis. Thus, Haynes et al. have shown that the rate constant for oxidative addition of MeI to  $\text{Rh}(\text{IME})_2(\text{CO})\text{I}$  (IME = 1,3-dimethylimidazol-2-ylidene) is ca. 3 times slower than the same reaction with  $\text{Rh}(\text{PEt}_3)_2(\text{CO})\text{I}$ , even though the NHC complex is the more electron rich of the two (on the basis of IR carbonyl stretching frequencies at 1943 and 1961  $\text{cm}^{-1}$ , respectively).<sup>2</sup> Furthermore, while the product of oxidative addition,  $\text{Rh}(\text{PEt}_3)_2$

$(\text{CO})\text{MeI}_2$ , can be isolated, the analogous NHC complex reacts further to give an equilibrium mixture of the acetyl complex  $\text{Rh}(\text{IME})_2(\text{COMe})\text{I}_2$  and  $\text{Rh}(\text{IME})_2(\text{CO})\text{I}$ . More recently, Crudden and co-workers<sup>3</sup> have shown that  $\text{Rh}(\text{IMes})(\text{PPh}_3)_2\text{Cl}$  (IMes = 1,3-bis(2,4,6-trimethylphenyl)imidazol-2-ylidene) not only undergoes slower intermolecular phosphine exchange than the parent phosphine species  $\text{Rh}(\text{PPh}_3)_3\text{Cl}$  but, surprisingly, dissociates IMes irreversibly in chlorinated solvent in the presence of excess phosphine.<sup>3</sup> Steric effects have been used to rationalize the different behaviors of the NHC and phosphine complexes in both cases. The use of this “steric factor” has been pushed to an even greater extreme with the isolation of a remarkable, air-stable 14-electron  $\text{RhL}(\text{CO})\text{Cl}$  species in which L is a cyclic alkyl(amino)carbene.<sup>4</sup>

We have recently reported that treatment of the rhodium hydride precursors  $\text{RhH}(\text{PPh}_3)_4$  and  $\text{RhH}(\text{PPh}_3)_3(\text{CO})$  with IMes,  $\text{I}^i\text{Et}_2\text{Me}_2$  (1,3-diethyl-4,5-dimethylimidazol-2-ylidene),  $\text{I}^i\text{Pr}_2\text{Me}_2$  (1,3-diisopropyl-4,5-dimethylimidazol-2-ylidene), or ICy (1,3-dicyclohexylimidazol-2-ylidene) leads to facile phosphine substitution, affording a range of mono- and bis-NHC rhodium(I) hydride complexes.<sup>5</sup> During the reaction of  $\text{RhH}(\text{PPh}_3)_3(\text{CO})$  with  $\text{I}^i\text{Pr}_2\text{Me}_2$ , we also obtained evidence for additional reaction pathways involving loss of hydride ligands with the isolation of the neutral dinuclear bridging carbonyl species  $(\text{PPh}_3)_2\text{Rh}(\mu\text{-CO})_2\text{Rh}(\text{I}^i\text{Pr}_2\text{Me}_2)_2$ . Herein, we report that the reactions of  $\text{RhH}(\text{PPh}_3)_3(\text{CO})$  with ICy in benzene, or  $\text{I}^i\text{Pr}_2\text{Me}_2$  in THF, also afford the stable, cationic tris-NHC complexes  $[\text{Rh}(\text{ICy})_3(\text{CO})]^+$  (**1**) and  $[\text{Rh}(\text{I}^i\text{Pr}_2\text{Me}_2)_3(\text{CO})]^+$  (**2**). The stability of **1** and **2** stands in stark contrast to the case for the analogous alkyl phosphine complexes, such as  $[\text{Rh}(\text{PMe}_3)_3(\text{CO})]^+$ , which remain uniso-

\* To whom correspondence should be addressed. E-mail: chsmkw@bath.ac.uk (M.K.W.).

<sup>†</sup> University of Bath.

<sup>‡</sup> ETHZ.

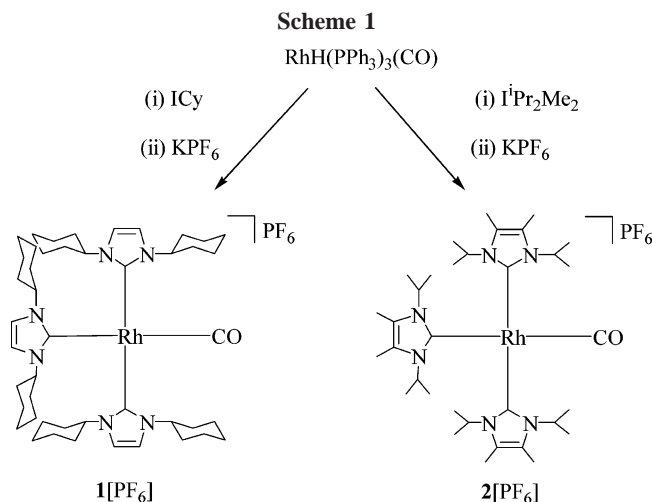
(1) (a) Chen, A. C.; Ren, L.; Decken, A.; Crudden, C. M. *Organometallics* **2000**, *19*, 3459. (b) Poyatos, M.; Mas-Marzá, E.; Mata, J.; Sanaú, M.; Peris, E. *Eur. J. Inorg. Chem.* **2003**, 1215. (c) Seo, H.; Kim, B. Y.; Lee, J. H.; Park, H.-J.; Son, S. U.; Chung, Y. K. *Organometallics* **2003**, *22*, 4783. (d) Mas-Marzá, E.; Poyatos, M.; Sanaú, M.; Peris, E. *Inorg. Chem.* **2004**, *43*, 2213. (e) Zarka, M. T.; Bortenschlager, M.; Wurst, K.; Nuyken, O.; Weberskirch, R. *Organometallics* **2004**, *23*, 4817. (f) Mas-Marzá, E.; Peris, E.; Castro-Rodríguez, I.; Meyer, K. *Organometallics* **2005**, *24*, 3158. (g) Mas-Marzá, E.; Sanaú, M.; Peris, E. *Inorg. Chem.* **2005**, *44*, 9961. (h) Bortenschlager, M.; Schütz, J.; von Preysing, D.; Nuyken, O.; Herrmann, W. A.; Weberskirch, R. *J. Organomet. Chem.* **2005**, *690*, 6233. (i) Imlinger, N.; Wurst, K.; Buchmeiser, M. R. *J. Organomet. Chem.* **2005**, *690*, 4433. (j) Andavan, G. T. S.; Bauer, E. B.; Letko, C. S.; Hollis, T. K.; Tham, F. S. *J. Organomet. Chem.* **2005**, *690*, 5938. (k) Chen, A. C.; Allen, D. P.; Crudden, C. M.; Wang, R.; Decken, A. *Can. J. Chem.* **2005**, *83*, 943. (l) Field, L. D.; Messerle, B. A.; Vuong, K. Q.; Turner, P. *Organometallics* **2005**, *24*, 4241. (m) Chianese, A. R.; Crabtree, R. H. *Organometallics* **2005**, *24*, 4432.

(2) Martin, H.; James, N. H.; Aitken, J.; Gaunt, J. A.; Adams, H.; Haynes, A. *Organometallics* **2003**, *22*, 4451.

(3) Allen, D. P.; Crudden, C. M.; Calhoun, L. A.; Wang, R. *J. Organomet. Chem.* **2004**, *689*, 3203.

(4) Lavallo, V.; Canac, Y.; DeHope, A.; Donnadiou, B.; Bertrand, G. *Angew. Chem., Int. Ed.* **2005**, *44*, 7236.

(5) Douglas, S.; Lowe, J. P.; Mahon, M. F.; Warren, J. E.; Whittlesey, M. K. *J. Organomet. Chem.* **2005**, *690*, 5027.



lated.<sup>6</sup> This stabilization must be due in part to the presence of sterically bulky *N*-substituents on the NHCs.

## Results and Discussion

**Formation and Structural Characterization of  $[\text{Rh}(\text{NHC})_3(\text{CO})]^+$ .** When THF or benzene solutions of  $\text{RhH}(\text{PPh}_3)_3(\text{CO})$  were allowed to react with  $\text{IPr}_2\text{Me}_2$  or ICy, yellow precipitates of the cationic tris-NHC complexes  $[\text{Rh}(\text{NHC})_3(\text{CO})]^+$  (NHC = ICy (**1**),  $\text{IPr}_2\text{Me}_2$  (**2**)) were deposited. The cationic metal fragments of compounds **1** and **2** were characterized by a combination of NMR and IR spectroscopy, although the corresponding anions proved to be unidentifiable. Upon crystallization and X-ray structural analysis, a range of quite random anions were identified, including  $[\text{PPh}_2\text{O}_2]^-$ . Stirring dichloromethane solutions of the isolated cations with aqueous solutions of  $\text{KPF}_6$  afforded **1** and **2** as the more reliable hexafluorophosphate salts, which were isolated in yields of 32 and 17%, respectively (Scheme 1).

The structures of **1**[PF<sub>6</sub>] and **2**[PF<sub>6</sub>], determined by X-ray crystallography, are shown in Figures 1 and 2, along with selected structural parameters; crystallographic data are given in Table 1. Both compounds display the expected distorted-square-planar geometries, with all three NHC ligands twisted out of the central plane defined by the Rh and the four coordinated carbon atoms. In both cases, the imidazole ring of the NHC ligand trans to CO forms a more acute angle (**1**[PF<sub>6</sub>], 52.3°; **2**[PF<sub>6</sub>], 52.9°) than the two trans ligands, which lie at 69.3 and 64.0° in the case of **1**[PF<sub>6</sub>] and at 67.0 and 63.6° in **2**[PF<sub>6</sub>]. Both structures reveal Rh–C<sub>NHC</sub> distances trans to CO that are significantly longer than the corresponding bond lengths to the two remaining, mutually trans NHC ligands (**1**[PF<sub>6</sub>], Rh–C(2) = 2.1321(12) Å, Rh–C(17) = 2.0638(11) Å, Rh–C(32) = 2.0642(11) Å; **2**[PF<sub>6</sub>], Rh–C(2) = 2.1490(13) Å, Rh–C(13) = 2.0738(14) Å, Rh–C(24) = 2.0775(13) Å). Perhaps the closest structurally characterized analogue, namely  $[\text{Rh}(\text{PPh}_3)_3(\text{CO})][\text{BF}_4]$ , shows quite different metrics, with the Rh–P distance to one of the two mutually trans phosphines being shorter than the other Rh–P distances.<sup>7</sup>

The IR spectra of **1**[PF<sub>6</sub>] and **2**[PF<sub>6</sub>] show carbonyl absorption bands at 1956 and 1953  $\text{cm}^{-1}$ , respectively, considerably lower than those found for  $[\text{Rh}(\text{PPh}_3)_3(\text{CO})][\text{HC}(\text{SO}_2\text{CF}_3)_2]$  (2026  $\text{cm}^{-1}$ )<sup>8</sup> and  $[\text{RhL}(\text{CO})][\text{PF}_6]$  (L = 2,6-bis(methylimidazol-2-

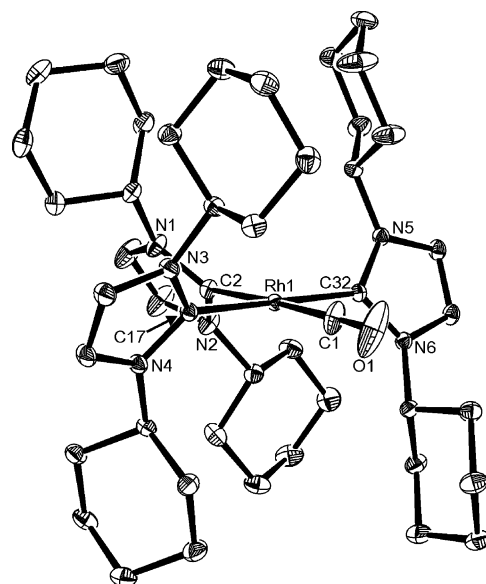


**Figure 1.** Molecular structure of the cation in  $[\text{Rh}(\text{ICy})_3(\text{CO})][\text{PF}_6]$  (**1**[PF<sub>6</sub>]). Thermal ellipsoids are shown at the 30% probability level. The hexafluorophosphate anion is omitted for clarity. Selected distances (Å) and angles (deg): Rh(1)–C(1) = 1.8322(15), Rh(1)–C(32) = 2.0642(11), Rh(1)–C(17) = 2.0638(11), Rh(1)–C(2) = 2.1321(12); C(1)–Rh(1)–C(2) = 177.86(7), C(17)–Rh(1)–C(32) = 177.39(5), C(32)–Rh(1)–C(2) = 91.60(5), C(17)–Rh(1)–C(2) = 90.93(5), C(1)–Rh(1)–C(32) = 89.05(6), C(1)–Rh(1)–C(17) = 88.44(6).

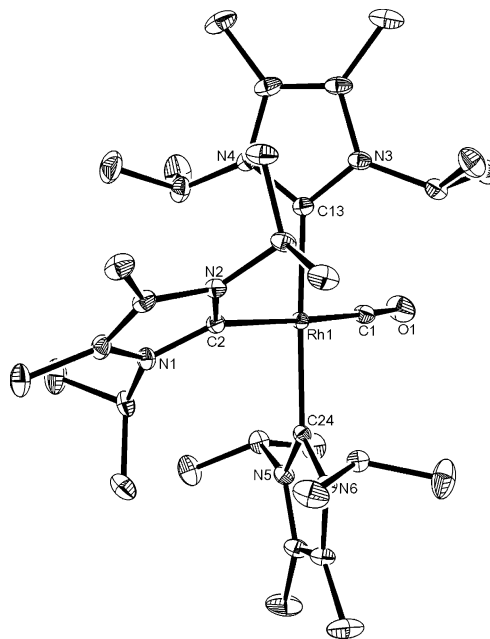


**Figure 2.** Molecular structure of the cation in  $[\text{Rh}(\text{IPr}_2\text{Me}_2)_3(\text{CO})][\text{PF}_6]$  (**2**[PF<sub>6</sub>]). Thermal ellipsoids are shown at the 30% probability level. The hexafluorophosphate anion is omitted for clarity. Selected distances (Å) and angles (deg): Rh(1)–C(1) = 1.8367(15), Rh(1)–C(24) = 2.0775(13), Rh(1)–C(13) = 2.0738(14), Rh(1)–C(2) = 2.1490(13); C(1)–Rh(1)–C(2) = 176.38(6), C(13)–Rh(1)–C(24) = 177.56(5), C(24)–Rh(1)–C(2) = 91.90(5), C(1)–Rh(1)–C(24) = 90.23(6), C(13)–Rh(1)–C(2) = 90.01(5), C(1)–Rh(1)–C(13) = 87.95(6).

ylidene)pyridine; 1982  $\text{cm}^{-1}$ ),<sup>9</sup> reflecting the strong  $\sigma$ -donor properties of the NHC ligands. Interestingly, given that NHCs

(6) Scott, S. L.; Szapkowicz, M.; Mills, A.; Santini, C. C. *J. Am. Chem. Soc.* **1998**, *120*, 1883.

(7) Clark, H. C. S.; Coleman, K. S.; Fawcett, J.; Holloway, J. H.; Hope, E. G.; Langer, J.; Smith, I. M. *J. Fluorine Chem.* **1998**, *91*, 207.

(8) Siedle, A. R.; Newmark, R. A.; Howells, R. D. *Inorg. Chem.* **1988**, *27*, 2473.

**Table 1.** Crystal Data and Structure Refinement Details for **1**[PF<sub>6</sub>], **2**[PF<sub>6</sub>], and **3**[PF<sub>6</sub>]

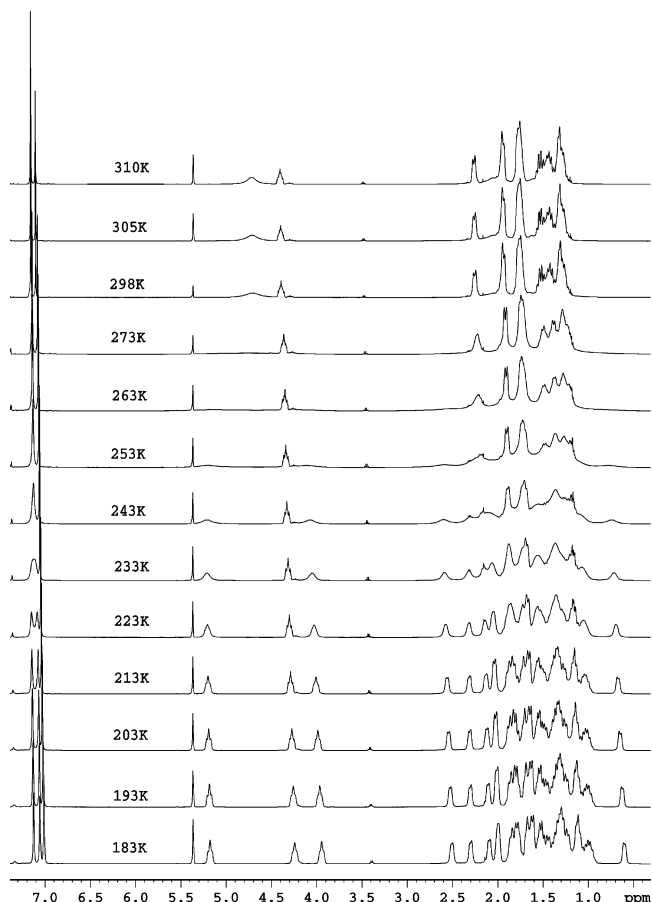
	<b>1</b> [PF <sub>6</sub> ]	<b>2</b> [PF <sub>6</sub> ]	<b>3</b> [PF <sub>6</sub> ]
empirical formula	C <sub>46</sub> H <sub>72</sub> F <sub>6</sub> N <sub>6</sub> OPRh	C <sub>34</sub> H <sub>60</sub> F <sub>6</sub> N <sub>6</sub> OPRh	C <sub>39</sub> H <sub>66</sub> Cl <sub>2</sub> F <sub>6</sub> N <sub>6</sub> OPRh
fw	972.98	816.76	953.76
cryst syst	monoclinic	triclinic	triclinic
space group	<i>P</i> 2 <sub>1</sub> / <i>c</i>	<i>P</i> 1 (No. 2)	<i>P</i> 1 (No. 2)
<i>a</i> /Å	15.0300(1)	9.9830(1)	10.5110(1)
<i>b</i> /Å	15.0630(1)	12.7140(1)	14.4190(1)
<i>c</i> /Å	21.6460(2)	16.4590(1)	15.4100(1)
$\alpha$ /deg		80.367(1)	84.158(1)
$\beta$ /deg	96.431(1)	76.200(1)	78.804(1)
$\gamma$ /deg		80.032(1)	86.557(1)
<i>U</i> /Å <sup>3</sup>	4869.75(6)	1980.69(3)	2277.22(3)
<i>Z</i>	4	2	2
<i>D<sub>c</sub></i> /g cm <sup>-3</sup>	1.327	1.369	1.391
<i>M</i> /mm <sup>-1</sup>	0.446	0.534	0.589
<i>F</i> (000)	2048	856	996
cryst size/mm	0.50 × 0.50 × 0.15	0.45 × 0.40 × 0.40	0.25 × 0.25 × 0.20
min, max $\theta$ /deg	3.65, 30.06	3.56, 30.91	3.53, 30.54
index ranges	-21 ≤ <i>h</i> ≤ 21; -21 ≤ <i>k</i> ≤ 21; -30 ≤ <i>l</i> ≤ 30	-14 ≤ <i>h</i> ≤ 14; -18 ≤ <i>k</i> ≤ 18; -22 ≤ <i>l</i> ≤ 23	-15 ≤ <i>h</i> ≤ 15; -20 ≤ <i>k</i> ≤ 20; -21 ≤ <i>l</i> ≤ 21
no. of rflns collected	86 647	40 529	47 613
no. of indep rflns, <i>R</i> (int)	14 144, 0.0397	12 310, 0.0399	13 880, 0.0351
no. of obsd rflns (>2 $\sigma$ )	12 777	11 164	12 834
no. of data/restraints/params	14 144/0/550	12 310/0/461	13 880/0/517
goodness of fit on <i>F</i> <sup>2</sup>	1.030	1.046	1.040
final <i>R</i> <sub>1</sub> , <i>wR</i> <sub>2</sub> indices ( <i>I</i> > 2 $\sigma$ ( <i>I</i> ))	0.0286, 0.0719	0.0306, 0.0743	0.0305, 0.0756
final <i>R</i> <sub>1</sub> , <i>wR</i> <sub>2</sub> indices (all data)	0.0331, 0.0755	0.0361, 0.0774	0.0348, 0.0778
largest diff peak and hole/e Å <sup>-3</sup>	0.478, -0.819	0.864, -0.846	0.883, -0.687

are generally accepted to be better donors than even the most donating phosphines,  $\nu_{\text{CO}}$  for the silica-supported  $\equiv\text{SiO}[\text{Rh}(\text{PMe}_3)_3\text{CO}]^+$  cation appears at lower frequency (1934 cm<sup>-1</sup>).<sup>6</sup>

**NMR Measurements on **1** and **2**.** The room-temperature <sup>1</sup>H NMR spectrum of **1**[PF<sub>6</sub>] reveals a number of broad signals in the aliphatic region for the Cy substituents and two signals, in the ratio 2:1, for the NCH=CHN protons. Further, one of the two observable methine resonances of the Cy groups, at ca. 4.5 ppm, is extremely broad, suggesting some form of fluxional behavior. A set of variable-temperature <sup>1</sup>H spectra for **1**[PF<sub>6</sub>] was measured, and these are shown in Figure 3. At 203 K, all of the signals are relatively sharp and reveal three nonequivalent signals, in the ratio 1:1:1, for both the Cy methine groups and the NCH=CHN backbone protons. A line shape analysis<sup>10</sup> of the data from Figure 3 affords an energy of activation of 35(±1) kJ mol<sup>-1</sup> for the two trans-positioned Rh-C<sub>NHC</sub> bonds. A similar set of NMR spectra were recorded for the salt **2**[PF<sub>6</sub>] (Figure 4) and, at 203 K, gave three nonequivalent signals for the <sup>1</sup>Pr methine resonances as well as three signals for the NCM=CMEN protons. The relative integrals within each group are again 1:1:1. For **2**[PF<sub>6</sub>], at 203 K one finds six nonequivalent <sup>1</sup>Pr methyl signals due to the three different sets of diastereotopic CH<sub>3</sub> protons. Analysis of the various line shapes afforded an energy of activation of 40(±1) kJ mol<sup>-1</sup> for the two mutually trans NHC ligands. The BAR<sub>4</sub><sup>F</sup> salt of **1** was prepared, and the variable-temperature study for this salt (see the Supporting Information) resulted in an activation energy of 38(±1) kJ mol<sup>-1</sup>. We do not observe any significant difference between the NMR spectra for **1**[PF<sub>6</sub>] and **1**[BAR<sub>4</sub><sup>F</sup>] in the regions of the carbene resonances, and we attribute the differences in the calculated energies to the experimental error.<sup>10</sup>

We believe that the observed temperature dependences in the salts **1**[PF<sub>6</sub>] and **2**[PF<sub>6</sub>] are a consequence of restricted rotation associated with the three Rh-C(carbene) bonds. At low temperature the three different sites are assigned as A-C for

the Cy-methine protons and a-c for the three NCH=CHN protons, as indicated in Chart 1. The two trans carbene ligands are not exactly perpendicular to the C-Rh-C plane defined by the OC-Rh-C(trans-carbene) fragment, with the result that the two N-substituents on the carbene reside in two different environments: i.e., one closer to the CO and the other proximate

**Figure 3.** <sup>1</sup>H NMR spectra (500 MHz) of [Rh(ICy)<sub>3</sub>(CO)][PF<sub>6</sub>] (**1**[PF<sub>6</sub>]) in CD<sub>2</sub>Cl<sub>2</sub> as a function of temperature.

(9) Wilson, J. M.; Sunley, G. L.; Adams, H.; Haynes, A. J. *Organomet. Chem.* **2005**, *690*, 6089.

(10) Sandstrom, J., *Dynamic NMR Spectroscopy*; Academic Press: London, 1982.

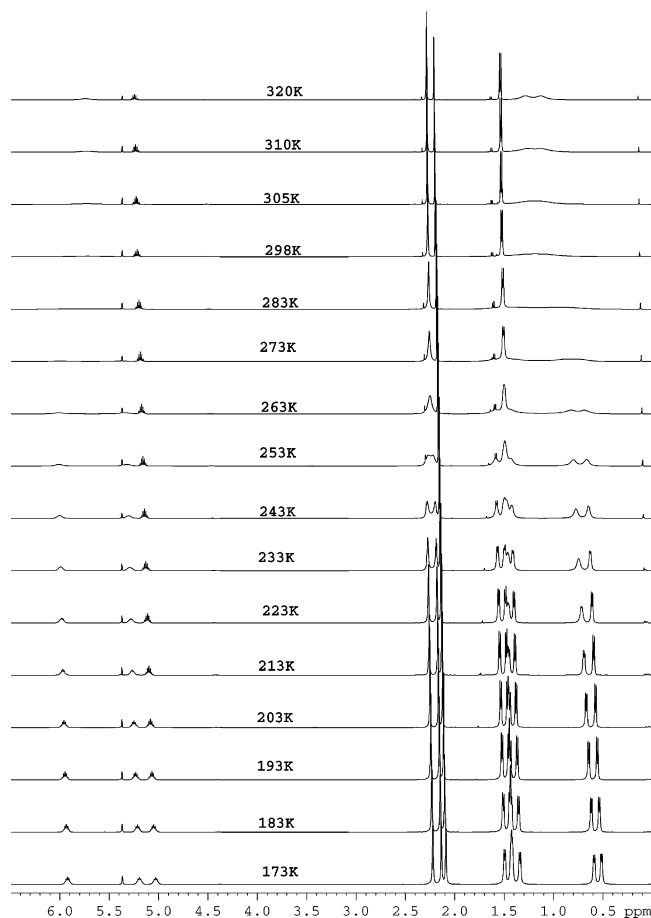


**Figure 4.**  $^1\text{H}$  NMR spectra (500 MHz) of  $[\text{Rh}(\text{IPr}_2\text{Me})_3(\text{CO})]^+[\text{PF}_6]^-$  ( $2[\text{PF}_6]$ ) in  $\text{CD}_2\text{Cl}_2$  as a function of temperature.

to the trans carbene ligand. Sections of the ROESY spectra<sup>11</sup> for  $1[\text{PF}_6]$  and  $2[\text{PF}_6]$  are shown in Figure 5 and reveal that, even at 203 K, there is slow exchange, e.g. in  $1[\text{PF}_6]$  between sites A and B.

We believe that the sites c and c' are also in exchange and that the entire process is concerted: i.e., all three carbene rings are rotating together. However, rotation of the imidazole ring in the NHC trans to the CO ligand moves the N-substituents into equivalent NMR environments, so that this exchange is not immediately recognized. However, a hint with respect to the rotation of this third ligand comes from the observed exchange between the diastereotopic  $^i\text{Pr}$  methyl groups within

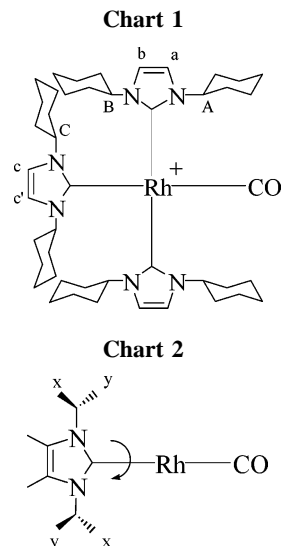


**Table 2.** PGSE Diffusion Data<sup>a</sup> for the Rh–NHC Salts  $1[\text{PF}_6]$ ,  $1[\text{BAR}_4\text{F}]$ , and  $2[\text{PF}_6]$

compd		$D$	$r_{\text{H}}$	$r_{\text{X-ray}}$ (Å)
$1[\text{PF}_6]$	cation	8.67	6.1	6.6
	anion	14.02	3.8	
$1[\text{BAR}_4\text{F}]$	cation	8.30	6.4	
	anion	8.32	6.4	
$2[\text{PF}_6]$	cation	9.33	5.7	6.2
	anion	14.70	3.6	

<sup>a</sup> Conditions: 400 MHz, 2 mM in  $\text{CH}_2\text{Cl}_2$ . Units:  $D$  values,  $10^{-10} \text{ m}^2 \text{ s}^{-1}$ ;  $r_{\text{H}}$  values, Å.  $\eta(\text{CH}_2\text{Cl}_2) = 0.414 \times 10^{-3} \text{ kg s}^{-1} \text{ m}^{-1}$  at 299 K.

the ring trans to the CO of  $2[\text{PF}_6]$ . These two methyl resonances, indicated as “x” and “y”, are well resolved ( $\delta$  0.52 and 1.33) and are also in slow exchange at 203 K on the basis of the ROESY data. We believe that this exchange process develops from the rotation indicated in Chart 2.

There are increasing indications of counterion effects on the kinetics of various homogeneously catalyzed reactions.<sup>12</sup> Changing the structure of a given cationic complex might well modify how the anion interacts. To probe this possibility, we have measured diffusion constants for three salts and show these data for  $1[\text{PF}_6]$ ,  $2[\text{PF}_6]$ , and  $1[\text{BAR}_4\text{F}]$  in  $\text{CH}_2\text{Cl}_2$  solution in Table 2. The results are derived from pulsed field gradient (PGSE) measurements, and we believe these to be the first diffusion measurements on *N*-heterocyclic carbene complexes. Diffusion constants from the individual ions of a salt are now recognized

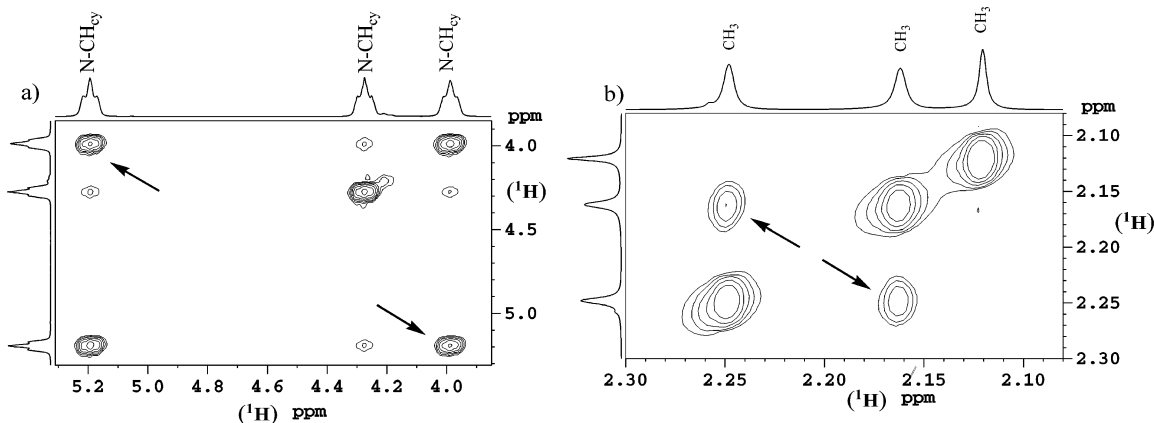


**Figure 5.** Sections of the ROESY spectra at 203 K for (left) the methine region of  $1[\text{PF}_6]$  and (right) the heterocyclic ring methyl groups for  $2[\text{PF}_6]$ . In both, the cross-peaks due to the exchange between the two sides of the trans carbene ligands are indicated with arrows ( $\text{CD}_2\text{Cl}_2$ , 500 MHz).

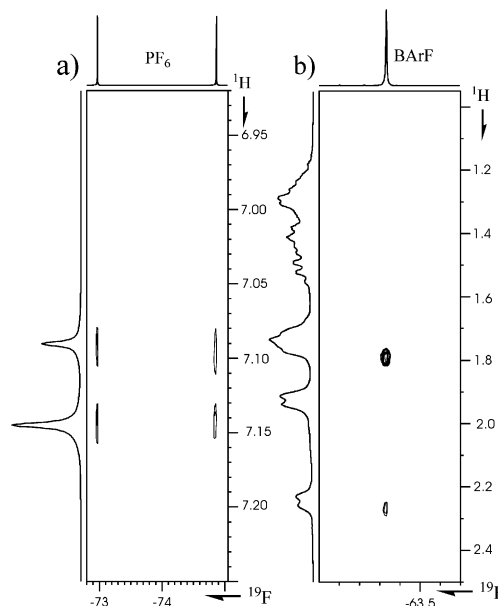


to reflect the degree of ion pairing.<sup>13,14</sup> As expected, on the basis of the X-ray data, the PF<sub>6</sub> anions reveal very much larger diffusion constants (*D* values) than the corresponding cation, so that for both **1**[PF<sub>6</sub>] and **2**[PF<sub>6</sub>] in CH<sub>2</sub>Cl<sub>2</sub>, there is not a substantial amount of ion pairing. Strong ion pairing would result in *D* values for the PF<sub>6</sub> anion which are close to or equal to that for the larger cation. The hydrodynamic radii, *r*<sub>H</sub>, for the cations, calculated from the Stokes–Einstein equation,<sup>15</sup> are slightly smaller than the radii calculated using the volume data from the crystallographic data.

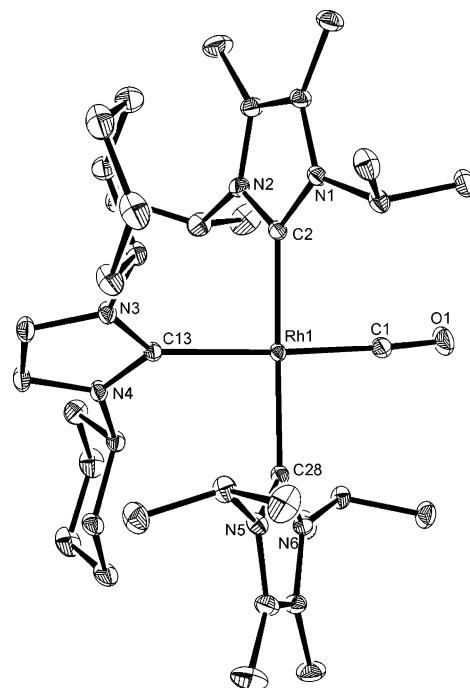
The BAR<sub>4</sub>F salt diffusion data are interesting, in that they represent a fairly rare example of measured identical *D* values for the two ions of a salt in the absence of strong ion pairing. By coincidence, the two ions in **1**[BAR<sub>4</sub>F] are of similar size and thus afford about the same *r*<sub>H</sub> values. A typical *r*<sub>H</sub> value for BAR<sub>4</sub>F in a polar solvent would be ca. 6 Å,<sup>16</sup> and the cation itself has an *r*<sub>H</sub> value of 6.1 Å. Allowing for perhaps 5–10% ion pairing readily explains the 6.4 Å *r*<sub>H</sub> values.

Figure 6 shows <sup>1</sup>H–<sup>19</sup>F HOESY results for **1**[PF<sub>6</sub>] and **1**[BAR<sub>4</sub>F]. The PF<sub>6</sub> anion, when it approaches the cation, does so via the NCH=CHN protons and avoids the Cy groups. The BAR<sub>4</sub>F anion, which is considerably larger than the PF<sub>6</sub> anion, cannot easily take the same pathway and thus reveals only modest contact to the methylene protons of the Cy substituents. For these two salts the size of the anion determines the proximity to the metal center.

**Isolation of [Rh(I<sup>t</sup>Pr<sub>2</sub>Me<sub>2</sub>)<sub>2</sub>(ICy)(CO)][PF<sub>6</sub>] (3[PF<sub>6</sub>]).** While the exact mechanism for formation of **1** and **2** remains to be fully elucidated, preliminary evidence suggests that dimeric species such as L<sub>2</sub>Rh(μ-CO)<sub>2</sub>Rh(NHC)<sub>2</sub> (L = PPh<sub>3</sub>, NHC) are possible intermediates in their formation. Addition of just over 1 equiv of ICy to a THF solution of (PPh<sub>3</sub>)<sub>2</sub>Rh(μ-CO)<sub>2</sub>Rh(I<sup>t</sup>Pr<sub>2</sub>Me<sub>2</sub>)<sub>2</sub> generated a yellow precipitate, which upon exchange with KPF<sub>6</sub> afforded a small amount of a microcrystalline solid that was characterized by <sup>1</sup>H NMR spectroscopy and X-ray diffraction as the mixed NHC cation [Rh(I<sup>t</sup>Pr<sub>2</sub>Me<sub>2</sub>)<sub>2</sub>(ICy)(CO)]<sup>+</sup>[PF<sub>6</sub>]<sup>-</sup> (**3**[PF<sub>6</sub>]). The cation structure is shown in Figure 7 and



**Figure 6.** Sections of the <sup>1</sup>H–<sup>19</sup>F HOESY results for (left) **1**[PF<sub>6</sub>] and (right) **1**[BAR<sub>4</sub>F]. In the PF<sub>6</sub> salt, there are only modest contacts to the NCH=CHN protons, whereas for the BAR<sub>4</sub>F salt, the selective contacts are now to CH<sub>2</sub> protons of the Cy groups (ambient temperature, CD<sub>2</sub>Cl<sub>2</sub>, 400 MHz).



**Figure 7.** Molecular structure of [Rh(ICy)(I<sup>t</sup>Pr<sub>2</sub>Me<sub>2</sub>)(CO)][PF<sub>6</sub>] (**3**[PF<sub>6</sub>]). Thermal ellipsoids are shown at the 30% probability level. The hexafluorophosphate anion is omitted for clarity. Selected distances (Å) and angles (deg): Rh(1)–C(1) = 1.8392(14), Rh(1)–C(28) = 2.0818(13), Rh(1)–C(2) = 2.0677(13), Rh(1)–C(13) = 2.1341(13); C(1)–Rh(1)–C(2) = 87.26(6), C(2)–Rh(1)–C(28) = 178.34(5), C(2)–Rh(1)–C(13) = 89.93(5), C(1)–Rh(1)–C(28) = 92.26(6), C(1)–Rh(1)–C(13) = 173.92(6), C(28)–Rh(1)–C(13) = 90.70(5).

shows the incorporation of the lone ICy ligand trans to CO. The structural parameters of the complex are similar to those of **1**[PF<sub>6</sub>] and **2**[PF<sub>6</sub>], although a slight difference in the two trans Rh–C<sup>I<sup>t</sup>Pr<sub>2</sub>Me<sub>2</sub></sup> bond lengths can be seen (2.0677(13) and 2.0818(13) Å).

(11) Hull, W. E. *Two-Dimensional NMR Spectroscopy. Applications for Chemists and Biochemists*; VCH: New York, 1987.

(12) (a) Fagnou, K.; Lautens, M. *Angew. Chem., Int. Ed.* **2002**, *41*, 27. (b) Smidt, S. P.; Zimmermann, N.; Studer, M.; Pfaltz, A. *Chem. Eur. J.* **2004**, *10*, 4685. (c) Kumar, P. G. A.; Pregosin, P. S.; Vallet, M.; Bernardinelli, G.; Jazzar, R. F.; Viton, F.; Kundig, E. P. *Organometallics* **2004**, *23*, 5410. (d) Faller, J. W.; Fontaine, P. P. *Organometallics* **2005**, *24*, 4132.

(13) (a) Zuccaccia, C.; Bellachioma, G.; Cardaci, G.; Macchioni, A. *Organometallics* **2000**, *19*, 4663. (b) Burini, A.; Fackler, J. P.; Galassi, R.; Macchioni, A.; Omary, M. A.; Rawashdeh-Omary, M. A.; Pietroni, B. R.; Sabatini, S.; Zuccaccia, C. *J. Am. Chem. Soc.* **2002**, *124*, 4570. (c) Zuccaccia, C.; Stahl, N. G.; Macchioni, A.; Chen, M. C.; Roberts, J. A.; Marks, T. J. *J. Am. Chem. Soc.* **2004**, *126*, 1448. (d) Macchioni, A. *Chem. Rev.* **2005**, *105*, 2039. (e) Zuccaccia, D.; Clot, E.; Macchioni, A. *New J. Chem.* **2005**, *29*, 430. (f) Song, F. Q.; Lancaster, S. J.; Cannon, R. D.; Schormann, M.; Humphrey, S. M.; Zuccaccia, C.; Macchioni, A.; Bochmann, M. *Organometallics* **2005**, *24*, 1315.

(14) (a) Kumar, P. G. A.; Pregosin, P. S.; Goicoechea, J. M.; Whittlesey, M. K. *Organometallics* **2003**, *22*, 2956. (b) Pregosin, P. S.; Martinez-Viviente, E.; Kumar, P. G. A. *Dalton Trans.* **2003**, 4007. (c) Martinez-Viviente, E.; Pregosin, P. S.; Vial, L.; Herse, C.; Lacour, J. *Chem. Eur. J.* **2004**, *10*, 2912. (d) Fernandez, I.; Martinez-Viviente, E.; Breher, F.; Pregosin, P. S. *Chem. Eur. J.* **2005**, *11*, 1495. (e) Pregosin, P. S.; Kumar, P. G. A.; Fernandez, I. *Chem. Rev.* **2005**, *105*, 2977. (f) Nama, D.; Kumar, P. G. A.; Pregosin, P. S. *Magn. Reson. Chem.* **2005**, *43*, 246.

(15) The Stokes–Einstein equation is  $D = (kT)/(\eta r_H)$ , where *k* is the Boltzmann constant, *T* the temperature, and *η* the viscosity of the solvent. This is not a completely reliable relation,<sup>13c,d</sup> but it does compensate for the solvent viscosity.

(16) (a) Drago, D.; Pregosin, P. S.; Pfaltz, A. *Chem. Commun.* **2002**, 286. (b) Schott, D.; Pregosin, P. S.; Jacques, N.; Chavarot, M.; Rose-Munch, F.; Rose, E. *Inorg. Chem.* **2005**, *44*, 5941. (c) Schott, D.; Pregosin, P. S.; Veiros, L. F.; Calhorda, M. J. *Organometallics* **2005**, *24*, 5710.

## Summary

The cationic *N*-heterocyclic carbene complexes  $[\text{Rh}(\text{NHC})_3(\text{CO})]^+$  (NHC = ICy,  $\text{IPr}_2\text{Me}_2$ ) have been isolated as the hexafluorophosphate salts and fully characterized by a combination of 1-D and 2-D NMR plus IR spectroscopy and X-ray diffraction. Variable-temperature  $^1\text{H}$  NMR studies reveal that there is restricted rotation about the three Rh–C<sub>NHC</sub> bonds in both complexes; low-temperature ROESY spectra indicate that this rotation occurs in a concerted manner. The isolation of the mixed NHC complex **3**[PF<sub>6</sub>], which is formed upon reaction of ICy with the neutral dimer  $(\text{PPh}_3)_2\text{Rh}(\mu\text{-CO})_2\text{Rh}(\text{IPr}_2\text{Me}_2)_2$ , suggests that additional studies into the mechanism of formation of these cationic complexes are warranted.

## Experimental Section

**General Comments.** All manipulations were carried out using standard Schlenk and glovebox techniques. Solvents were purified using an MBraun SPS solvent system (pentane, THF, dichloromethane) or under a nitrogen atmosphere from purple solutions of sodium benzophenone ketyl (benzene). CD<sub>2</sub>Cl<sub>2</sub> (Aldrich) was vacuum-transferred from CaH<sub>2</sub>.  $\text{RhH}(\text{PPh}_3)_3(\text{CO})$ ,  $\text{IPr}_2\text{Me}_2$ , and  $\text{BAR}_4\text{F}$  were prepared using literature routes,<sup>17–19</sup> while ICy was prepared according to a method described by Nolan.<sup>20</sup>

NMR spectra were recorded on Bruker Avance 400 and 500 MHz NMR spectrometers and referenced to the dichloromethane solvent signals ( $^1\text{H}$ ,  $\delta$  5.32;  $^{13}\text{C}\{^1\text{H}\}$ ,  $\delta$  53.73).  $^{31}\text{P}\{^1\text{H}\}$  NMR chemical shifts were referenced externally to 85% H<sub>3</sub>PO<sub>4</sub> ( $\delta$  0.0). 2-D experiments ( $^1\text{H}$  COSY,  $^1\text{H}$ –X (X =  $^{13}\text{C}$ ,  $^{31}\text{P}$ ) HMQC/HMBC, EXSY, NOESY) were performed using standard Bruker pulse sequences. IR spectra were recorded as Nujol mulls on a Nicolet Protégé 460 FTIR spectrometer. Elemental analyses were performed by Elemental Microanalysis Ltd, Okehampton, Devon, U.K.

All of the diffusion measurements were performed on a 400 MHz Bruker AVANCE spectrometer equipped with a microprocessor-controlled gradient unit and an inverse multinuclear probe with an actively shielded Z-gradient coil. The shape of the gradient pulses was rectangular, their lengths were 1.75 ms and their strength were incremented in 4% steps, so that 10–15 points could be used for regression analysis. The time between the midpoints of the gradients ( $\Delta$ ) was chosen as 167.75 ms. The measurements were carried out without sample spinning and in the absence of external air flow. For  $^{19}\text{F}$ ,  $T_1$  was always determined before the measurement and the recovery delay  $D_1$  set to  $5T_1$ . For  $^1\text{H}$ ,  $D_1$  was set to 5 s. The experiments were carried out at a set temperature of 299 K within the NMR probe. The concentration used for the measurements was 2 mM. The error coefficient for the  $D$  values on the basis of our experience is  $\pm 0.06$ .

The  $^1\text{H}$ – $^{19}\text{F}$  HOESY measurements were performed on a 400 MHz Bruker AVANCE spectrometer equipped with a doubly tuned ( $^1\text{H}$ ,  $^{19}\text{F}$ ) TXI probe. A mixing time of 800 ms was used at a set temperature of 299 K within the NMR probe. The concentration of the sample was 10 mM in CD<sub>2</sub>Cl<sub>2</sub>. The variable-temperature NMR spectra and 2D experiments were recorded on a Bruker Avance 500 MHz spectrometer.  $^1\text{H}$ – $^1\text{H}$  ROESY was performed using the standard Bruker pulse sequence with a mixing time of 250 ms at a set temperature of 203 K within the NMR probe.

The rate constants derived from the variable-temperature data are extracted by fitting the calculated line shape to the experiment. This was done by manual iteration and visual comparison. The iterative program Mexico (version 3) was used.<sup>21</sup> Line shape

analysis over the temperature range 298–203 K gave a set of rate constants, and the resulting plot of  $\ln k$  vs  $1/T$  afforded the activation parameter  $E_A$  from the Arrhenius equation.

**$[\text{Rh}(\text{ICy})_3(\text{CO})][\text{PF}_6]$ .** Addition of ICy (0.34 g, 1.46 mmol) to a benzene solution (10 mL) of  $\text{RhH}(\text{PPh}_3)_3(\text{CO})$  (0.22 g, 0.24 mmol) resulted in the formation of a yellow precipitate upon stirring for 90 min. The yellow solid was isolated by cannula filtration, dissolved in CH<sub>2</sub>Cl<sub>2</sub> (3 mL), and treated with an aqueous solution (2 mL) of KPF<sub>6</sub> (0.23 g, 1.25 mmol). After 30 min of vigorous stirring, the aqueous layer was removed by cannula and the organic phase dried over MgSO<sub>4</sub> and filtered. Subsequent layering of the filtrate with pentane afforded yellow crystals of **1**[PF<sub>6</sub>] (yield 75 mg, 32%). Anal. Found (calcd) for  $\text{RhC}_4\text{H}_7\text{N}_6\text{OPF}_6$ : C, 56.28 (56.78); H, 7.32 (7.46); N, 8.46 (8.64).  $^1\text{H}$  NMR (CD<sub>2</sub>Cl<sub>2</sub>, 500 MHz, 203 K):  $\delta$  7.09 (s, 2H, NCH=CHN), 7.02 (s, 2H, NCH=CHN), 6.98 (s, 2H, NCH=CHN), 5.15 (m, 2H, NCH<sub>cyclohexyl</sub>), 4.23 (m, 2H, NCH<sub>cyclohexyl</sub>), 3.94 (m, 2H, NCH<sub>cyclohexyl</sub>), 2.49 (m, 2H, CH<sub>2</sub>), 2.26 (m, 2H, CH<sub>2</sub>), 2.07 (m, 2H, CH<sub>2</sub>), 1.98 (m, 4H, CH<sub>2</sub>), 1.84–0.93 (m, 48H, CH<sub>2</sub>), 0.60 (m, 2H, CH<sub>2</sub>).  $^{13}\text{C}\{^1\text{H}\}$  NMR (CD<sub>2</sub>Cl<sub>2</sub>, 126 MHz, 203 K):  $\delta$  190.8 (d,  $J_{\text{CRh}}$  = 62.9 Hz, Rh–CO), 179.8 (d,  $J_{\text{CRh}}$  = 42.2, Rh–C<sub>ICy</sub>), 177.7 (d,  $J_{\text{CRh}}$  = 46.1 Hz, Rh–C<sub>ICy</sub>), 118.2 (s, NCH=CHN), 117.6 (s, NCH=CHN), 117.5 (s, NCH=CHN), 60.1 (s, NCH<sub>cyclohexyl</sub>), 59.0 (s, NCH<sub>cyclohexyl</sub>), 57.8 (s, NCH<sub>cyclohexyl</sub>), 35.9 (s, CH<sub>2</sub>), 34.4 (s, CH<sub>2</sub>), 34.0 (s, CH<sub>2</sub>), 33.4 (s, CH<sub>2</sub>), 33.0 (s, CH<sub>2</sub>), 32.8 (s, CH<sub>2</sub>), 30.6 (s, CH<sub>2</sub>), 25.3 (s, CH<sub>2</sub>), 25.1 (s, CH<sub>2</sub>), 24.7 (s, CH<sub>2</sub>), 24.6 (s, CH<sub>2</sub>), 24.4 (s, CH<sub>2</sub>), 24.1 (s, CH<sub>2</sub>), 24.0 (s, CH<sub>2</sub>), 23.8 (s, CH<sub>2</sub>). IR (cm<sup>–1</sup>): 1956 ( $\nu_{\text{CO}}$ ).

$[\text{Rh}(\text{ICy})_3(\text{CO})][\text{BAR}_4\text{F}]$  was prepared by adding 1 equiv of NaBAR<sub>4</sub>F (32 mg, 36  $\mu\text{mol}$ ) to **1**[PF<sub>6</sub>] (35 mg, 36  $\mu\text{mol}$ ) in CH<sub>2</sub>Cl<sub>2</sub> (1 mL). After 1 h, the mixture was filtered and the volatiles were removed, affording **1**[BAR<sub>4</sub>F] as a yellow solid.  $^1\text{H}$  and  $^{13}\text{C}\{^1\text{H}\}$  NMR spectra displayed resonances for the ICy ligands almost identical with those seen for **1**[PF<sub>6</sub>].

**$[\text{Rh}(\text{IPr}_2\text{Me}_2)_3(\text{CO})][\text{PF}_6]$ .**  $\text{IPr}_2\text{Me}_2$  (0.24 g, 1.31 mmol) and  $\text{RhH}(\text{PPh}_3)_3(\text{CO})$  (0.20 g, 0.22 mmol) were dissolved in THF (10 mL), and the mixture was stirred for 30 min. The dark solution was layered with hexane, from which a mixture of yellow and red crystals grew (the red crystals were identified as  $(\text{PPh}_3)_2\text{Rh}(\mu\text{-CO})_2\text{Rh}(\text{IPr}_2\text{Me}_2)_2$ ).<sup>5</sup> The yellow crystals were separated and dissolved in CH<sub>2</sub>Cl<sub>2</sub> (3 mL) and treated as outlined above for **1**. The complex **2**[PF<sub>6</sub>] was isolated as a yellow microcrystalline solid (yield 30 mg, 17%). Crystals suitable for X-ray crystallography were grown from CH<sub>2</sub>Cl<sub>2</sub>/pentane. Anal. Found (calcd) for  $\text{RhC}_3\text{H}_6\text{N}_6\text{OPF}_6$ : C, 50.00 (49.94); H, 7.40 (7.33); N, 10.29 (10.18).  $^1\text{H}$  NMR (CD<sub>2</sub>Cl<sub>2</sub>, 500 MHz, 203 K):  $\delta$  5.90 (sept,  $J_{\text{HH}}$  = 6.94 Hz, 2H, CHMe<sub>2</sub>), 5.20 (sept,  $J_{\text{HH}}$  = 7.11 Hz, 2H, CHMe<sub>2</sub>), 5.03 (sept,  $J_{\text{HH}}$  = 7.11 Hz, 2H, CHMe<sub>2</sub>), 2.20 (s, 6H, MeC=CMe), 2.11 (s, 6H, MeC=CMe), 2.07 (s, 6H, MeC=CMe), 1.49 (d,  $J_{\text{HH}}$  = 6.94 Hz, 6H, NCHMe), 1.42 (d,  $J_{\text{HH}}$  = 6.94 Hz, 6H, NCHMe), 1.39 (d,  $J_{\text{HH}}$  = 7.11 Hz, 6H, NCHMe), 1.33 (d,  $J_{\text{HH}}$  = 7.11 Hz, 6H, NCHMe), 0.62 (d,  $J_{\text{HH}}$  = 7.11 Hz, 6H, NCHMe), 0.52 (d,  $J_{\text{HH}}$  = 7.11 Hz, 6H, NCHMe).  $^{13}\text{C}\{^1\text{H}\}$  NMR (CD<sub>2</sub>Cl<sub>2</sub>, 126 MHz, 203 K):  $\delta$  191.4 (d,  $J_{\text{CRh}}$  = 63.3 Hz, Rh–CO), 179.2 (d,  $J_{\text{CRh}}$  = 46.8 Hz, Rh–C<sub>IPr<sub>2</sub>Me<sub>2</sub></sub>), 178.3 (d,  $J_{\text{CRh}}$  = 43.2 Hz, Rh–C<sub>IPr<sub>2</sub>Me<sub>2</sub></sub>), 125.6 (s, MeC=CMe), 125.2 (s, MeC=CMe), 124.8 (s, MeC=CMe), 53.5 (s, NCHMe), 52.9 (s, NCHMe), 21.7 (s, NCHMe), 21.0 (s, NCHMe), 20.0 (s, NCHMe), 19.9 (s, NCHMe), 19.8 (s, NCHMe), 19.7 (s, NCHMe), 10.2 (s, MeC=CMe), 10.1 (s, MeC=CMe). IR (cm<sup>–1</sup>): 1953 ( $\nu_{\text{CO}}$ ).

**$[\text{Rh}(\text{IPr}_2\text{Me}_2)_2(\text{ICy})(\text{CO})][\text{PF}_6]$ .**  $(\text{PPh}_3)_2\text{Rh}(\mu\text{-CO})_2\text{Rh}(\text{IPr}_2\text{Me}_2)_2$  (0.01 g, 0.008 mmol) and ICy (0.002 g, 0.011 mmol) were dissolved in *d*<sub>8</sub>-THF (0.6 mL) in a J. Young resealable NMR tube. A reaction was observed immediately at room temperature by  $^{31}\text{P}$  NMR, and after a few days at room temperature, a yellow solid had precipitated out. This was dissolved in CD<sub>2</sub>Cl<sub>2</sub> (0.6 mL), a

(17) Ahmad, N.; Levison, J. J.; Robinson, S. D.; Uttley, M. F. *Inorg. Synth.* **1990**, 28, 81.

(18) Kühn, N.; Kratz, T. *Synthesis* **1993**, 561.

(19) Buschman, W. E.; Miller, J. S. *Inorg. Synth.* **2002**, 33, 85.

(20) Nolan, S. P. Personal communication.

(21) Mexico (The McMaster program for exchange line shape calculations, version 3, by A. D. Bain, 2002).

degassed solution of  $\text{KPF}_6$  (0.01 g) in deionized water (2 mL) was added, and the mixture was vigorously shaken. The water was removed by cannula and the solution layered with pentane (2 mL). A few small, bright yellow crystals of  $\mathbf{3}[\text{PF}_6]$  were formed, which proved suitable for X-ray diffraction.  $^1\text{H}$  NMR ( $\text{CD}_2\text{Cl}_2$ , 400 MHz, 298 K):  $\delta$  7.08 (s, 2H,  $\text{NCH}=\text{CHN}$ ), 5.59 (sept,  $J_{\text{HH}} = 7.1$  Hz, 4H,  $\text{NCHMe}_2$ ), 4.47 (br m, 2H,  $\text{NCH}_{\text{cyclohexyl}}$ ), 2.23 (s, 12H,  $\text{NCMe}=\text{NCMe}$ ), 1.79–1.67 (m, 6H,  $\text{CH}_2$ ), 1.47 (d,  $J_{\text{HH}} = 7.1$  Hz, 12H,  $\text{NCHMe}_2$ ), 1.43–1.29 (m, 14H,  $\text{CH}_2$ ), 1.28 (d,  $J_{\text{HH}} = 7.1$  Hz, 12H,  $\text{NCHMe}_2$ ). IR ( $\text{cm}^{-1}$ ): 1956 ( $\nu_{\text{CO}}$ ).

**X-ray Crystallography.** Single crystals of compounds  $\mathbf{1}[\text{PF}_6]$ ,  $\mathbf{2}[\text{PF}_6]$ , and  $\mathbf{3}[\text{PF}_6]$  were analyzed at 150(2) K using graphite-monochromated Mo  $\text{K}\alpha$  radiation and a Nonius Kappa CCD diffractometer. Details of the data collections, solutions, and refinements are given in Table 1. The structures were uniformly solved using SHELXS-97<sup>22</sup> and refined using full-matrix least squares in SHELXL-97.<sup>22</sup> Convergence was uneventful, with only  $\mathbf{3}[\text{PF}_6]$  containing lattice solvent in the guise of one molecule of dichloromethane per asymmetric unit. Multiscan absorption cor-

rections were applied throughout. The maximum and minimum transmission factors for  $\mathbf{1}[\text{PF}_6]$ ,  $\mathbf{2}[\text{PF}_6]$ , and  $\mathbf{3}[\text{PF}_6]$  were respectively 0.88 and 0.78, 0.82 and 0.70, and 0.90 and 0.85. Crystallographic data for all three compounds have been deposited with the Cambridge Crystallographic Data Centre as supplementary publications CCDC 299790–299792. Copies of the data can be obtained free of charge on application to the CCDC, 12 Union Road, Cambridge CB2 1EZ, U.K. (fax, (+44) 1223 336033; e-mail, deposit@ccdc.cam.ac.uk).

**Acknowledgment.** M.K.W. thanks the EPSRC (S.B., S.D.), and P.S.P. thanks the Swiss National Science Foundation and the ETHZ for funding. We also thank Johnson Matthey plc for the loan of hydrated  $\text{RhCl}_3$ .

**Supporting Information Available:** X-ray crystallographic data as CIF files for complexes  $\mathbf{1}[\text{PF}_6]$ ,  $\mathbf{2}[\text{PF}_6]$ , and  $\mathbf{3}[\text{PF}_6]$ , tables and figures giving rate constants and Arrhenius plots associated with the variable-temperature proton measurements, and a figure showing the variable-temperature proton measurements for  $\mathbf{1}[\text{BAr}_4^{\text{F}}]$ . This material is available free of charge via the Internet at <http://pubs.acs.org>.

OM060202P

(22) Sheldrick, G. M. *Acta Crystallogr.* **1990**, *A46*, 467–473. Sheldrick, G. M. SHELXL-97, a Computer Program for Crystal Structure Refinement; University of Göttingen, Göttingen, Germany, 1997.